

# STATUS OF TESTING AND COMMISSIONING OF THE MEDIUM ENERGY BEAM TRANSPORT LINE OF THE ESS NORMAL CONDUCTING LINAC

A. Garcia Sosa<sup>†</sup>, R. Baron, H. Danared, C. Derrez, E. Donegani, M. Eshraqi, V. Grishin, A. Jansson, M. Jensen, B. Jones, E. Laface, B. Lagoguez, Y. Levinsen, J. Martins, N. Milas, R. Miyamoto, D. Nicosia, D. Noll, C. Plostinar, T. Shea, R. Tarkeshian, C. Thomas, E. Trachanas, P. van Velze, R. Zeng, ESS, Lund, Sweden  
 I. Bustinduy, A. Conde, D. Fernandez-Cañoto, N. Garmendia, P.J. Gonzalez, G. Harper, A. Kaftoosian, J. Martin, I. Mazkarian, J.L. Muñoz, A.R. Páramo, S. Varnasseri, A. Zugaza, ESS-Bilbao, Bilbao, Spain

## Abstract

The latest beam commissioning phase of the Normal Conducting LINAC at ESS delivered a proton beam through the Medium Energy Beam Transport (MEBT) into the first Drift Tube LINAC (DTL) tank. The probe beam in MEBT consisted of 3.6 MeV protons of <6 mA, <5 μs pulse length and 1 Hz repetition rate. Following the delivery of the components at ESS in Lund in June 2019, the commissioning phase with the MEBT was completed in July 2022. In March 2022, the maximum beam current of 62.5 mA was transported up to the MEBT Faraday cup. This proceeding focuses on the status of MEBT including magnets, buncher cavities, scrapers and beam diagnostics designed and tested in collaboration with ESS Bilbao.

## NORMAL CONDUCTING LINAC

The ESS LINAC starts with a Microwave Discharge Ion Source (MDIS). This source is capable of producing a 75 keV, 74 mA proton beam with a pulse length of 6 ns and 14 Hz repetition rate. An extraction system with a repeller electrode is employed to limit the back-streaming electrons [1]. The LEBT at ESS is roughly 2.5 m long and consists of two focusing solenoids with a pair of corrector magnets embedded in each of them, an iris with a changeable aperture is used to limit the beam current, a diagnostics tank with a pair of Allison emittance probes, a Faraday cup, and an electrostatic chopper. Two sets of Non-invasive Profile Monitors (NPMs) measure beam size and position and a Doppler monitor that measures the proton fraction. A collimator cone sits at the end of the LEBT as an interface with the RFQ. The IS and the LEBT are in-kind contributions from INFN Catania in Italy [2,3].

The beam dynamics design of the Radio Frequency Quadrupole (RFQ) is optimized for minimal losses and high beam quality in terms of transverse and longitudinal emittance [4]. The RFQ is an in-kind contribution from CEA [5].

The MEBT is described in the next section, and after that begins the DTL section, another successful in-kind

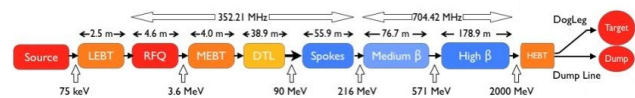


Figure 1: ESS LINAC.

contribution from INFN Legnaro [6]. The 39 m long DTL section is designed to accelerate the proton beam from 3.6 MeV to 90 MeV at a frequency of 352.21 MHz (see Fig. 1).

## MEBT

The MEBT section, located between the RFQ and the DTL tanks, focuses the beam transversally and longitudinally, and chops the beam pulse as it is transported down the LINAC. A schematic of the ESS MEBT is shown in Fig. 2.

The Medium Energy Beam Transport (MEBT) has several functions. It matches the RFQ output beam characteristics to the DTL input both transversally and longitudinally. The transverse focusing and matching is achieved with quadrupole magnets whereas the longitudinal matching is achieved with buncher cavities. Moreover, the beam trajectory correction is done by steering magnets. A stripline chopper removes longitudinal edges of the beam pulse, and subsequently the chopped beam is intercepted by a beam dump.

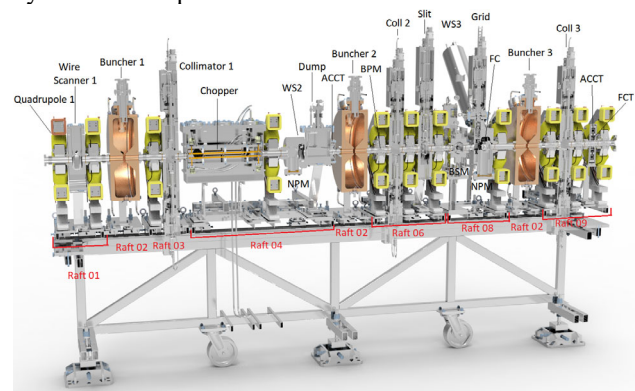


Figure 2: Schematic of the ESS MEBT.

Diagnostic instruments are used to measure a wide range of beam parameters, such as the beam matching and

<sup>†</sup>Alejandro.sosa@es.eu

position, the transverse beam emittance and profile, and the beam current.

## QUADRUPOLE MAGNETS

There are 11 quadrupole magnets with integrated horizontal and vertical corrector coils along the MEBT, as shown in Figs. 2 and 3. The magnets are designed to operate in DC and have water-cooled coils (see Fig. 3). The magnet aperture diameter is 41 mm and the beam pipe inner diameter is 36.8 mm. The quadrupole can produce and integrated magnetic field from 0.14 to 2.91 T at excitation currents ranging from 10 to 250 A. Two corrector magnets (steerers) can generate small vertical and horizontal kicks of up to 3.8 mT·m at 8.5 A when quadrupole field is off, and of up to 2 mT·m when the quadrupole field is at its maximum [7].

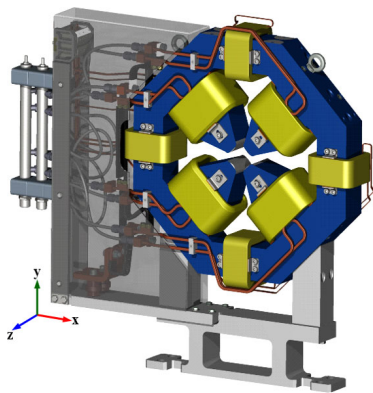


Figure 3: Quadrupole magnet with corrector coils.

The initial hardware testing phase proved useful in identifying leaking cooling connections, reversed polarity electrical connections, short-circuits due to confined longitudinal space and fine mechanical alignment issues. During the beam commissioning phase, the main issues found were input/output controller resets, one power supply failure and missing software functions that were added to the user interface.

The magnets follow a FODO lattice except quads 4 and 5 which are both focusing. In Fig. 4, a screenshot shows the interface to control the MEBT magnets. All the values shown are the design values for each magnet.

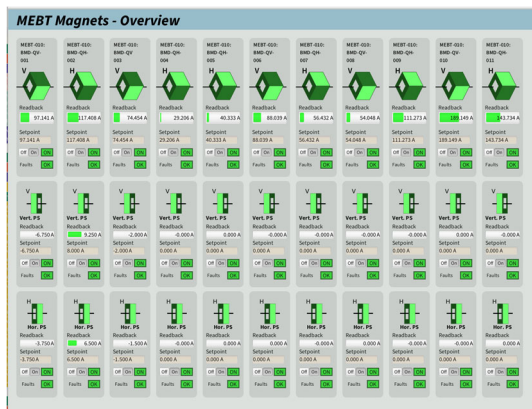


Figure 4: MEBT magnets overview screen.

## CHOPPER

The MEBT Chopper system includes the Chopper Stripline, Positive/Negative Pulsers, and corresponding cables and loads, which are all matched in order to prevent reflections and amplitude overshoots/undershoots. In order to chop the edges of the macro-pulse and reduce the rise and fall time of the 3.6 MeV proton beam of the MEBT, a stripline chopper was developed.

The design concept is based on the travelling wave stripline scheme. In this scheme the electromagnetic wave which is generated at the input port of stripline gap travels downstream and produces an electric and magnetic field which causes the required integrated deflection of the beam. The deflected beam is intercepted and absorbed by a beam dump located downstream. The overall rise/fall time of the Chopper system was measured to be less than 7 ns, which exceeds the specification. The beam macro-pulse injected into the MEBT has a rise and fall time considerably larger than the required 10 ns. The deflection of the beam is in the vertical plane and the nominal deflecting angle of the beam at the MEBT energy is 13.84 mrad.

Table 1: ESS MEBT Chopper Specifications

Parameter	Value
Deflector Type	TEM stripline
Beam energy	3.6 MeV
Stripline gap	20 mm
Deflection angle	13.84 mrad
Deflector length	450 mm
Total nominal deflecting voltage	4.5 kV (max. 5.2 kV)
Characteristic impedance	50 Ω
Good field region (GFR)	± 15 mm
Field flatness in GFR	<10%
Rise/fall time	≤10 ns (10-90%)
Nominal pulse length	1-20 μs
Beam abort pulse length	200 μs
Repetition rate	1-14 Hz
Time between chopping pulses	5 μs – 2.86 ms

The chopper beam dump is designed for operation withstanding pulses of 40 μs, which is considered a conservative value, since in nominal mode, two pulses of 20 μs separated by a time that varies from 50 μs to 2.86 ms will impact the beam dump. It also has to be capable of withstanding beam abort pulses of 200 μs in the event of LEBT chopper failure. The beam dump is made of a TZM plate with a length of 150 mm, and a width of 60 mm. The plate is separated from the axis by 18.4 mm at the entrance and 7 mm at the exit with an inclination of 4.35°. The chopper beam dump is placed in a vacuum vessel downstream.

## BUNCHER CAVITIES

The MEBT has 3 buncher cavities resonating at the frequency of 352.21 MHz. The cavity length is 126 mm and the beam aperture diameter is 30 mm. The main components of the buncher cavities are shown in Fig. 5. The cavity tuning system is based on two tuners. The first one is fixed and aimed to correct mechanical errors, and the second one is movable and controlled by the frequency loop of the LLRF system. This loop corrects the frequency drifts during the beam operation, assuring the cavity resonant condition. One loop type power coupler injects the RF power into the cavity. The maximum RF peak power is 22.5 kW and the maximum gap voltage is 150 kV [8].

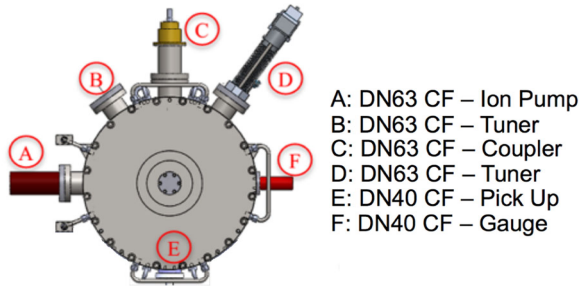


Figure 5: Transverse view of a MEBT buncher cavity showing all the ports.

The buncher cavities have been conditioned at ESS Bilbao and subsequently delivered and installed in Lund. All MEBT buncher cavities have been operated with closed loop LLRF operation. The tuners move in 0.2 mm steps if the frequency shifts more than  $\pm 3$  kHz. Buncher 1 is phased at 2.80 rad, buncher 2 at 2.02 rad and buncher 3 at -0.55 rad. These values correspond to  $-90^\circ$  phase with respect to the bunch. During the MEBT commissioning phase, issues related to cavity detuning, the Solid-State Power Amplifiers (SSPAs) and the LLRF were resolved. A tuner control script was developed following the cavity detuning limiting the tuner movement range to  $\pm 10$  mm [9].

A phase scan was performed for each cavity by changing the RF phase and comparing it against two BPMs after calibration [10], as shown in Fig. 6.

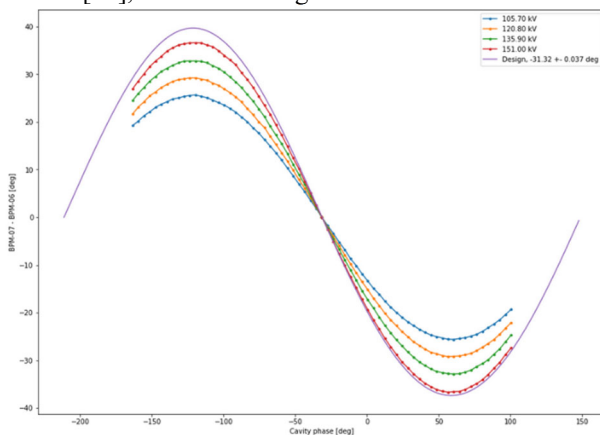


Figure 6: Buncher 3 phase scan against the MEBT BPM at different cavity voltages.

The beam is used to find which relative phase of the amplifier RF corresponds to  $90^\circ$  bunching phase. In Fig. 6 this is where the curves at different cavity fields overlap. In terms of amplitude, a model was fit, where the design curve is the solid line. This means we need a little bit higher fields in the cavity than the design value to get the BPM (or ToF) response we expect. It is also interesting how similar phase results we get from looking at different BPM pairs for example, and how this stability behaves over time.

## BEAM DIAGNOSTICS

The MEBT is equipped with a suite of beam instrumentation devices to measure the beam current in addition to transverse and longitudinal properties of the beam. Furthermore, it provides the means to collimate the beam in the transverse plane using three vertical scrapers. The main diagnostics devices deployed during this phase were the Faraday cup [11], the slit-grid emittance meter, the BPMs located inside the quadrupole magnet beam pipes, the three wire scanners and the ACCTs.

Most of the verifications with beam and beam dynamics studies were performed between November 2021 and February 2022 with probe beam ( $< 6$  mA,  $< 5$   $\mu$ s and 1 Hz). On 12-March-2022 the maximum proton current was transported up to the MEBT FC (Fig.7 shows the first ramp-up to 62.6 mA). The MEBT FC was used as a beam dump through the MEBT commissioning.

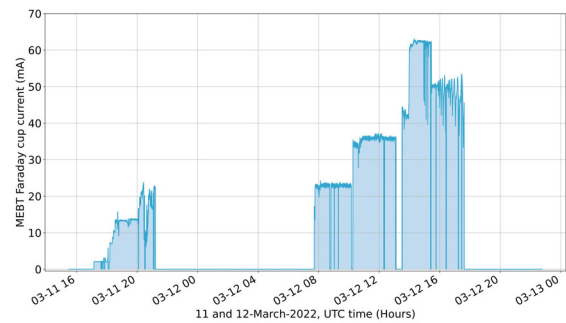


Figure 7: Maximum proton current measured by the MEBT Faraday cup.

Not yet available at this stage were the signal acquisition system of the scrapers, the Bunch Shape Monitor (BSM) and the NPM cameras to measure transverse beam size and position.

## CONCLUSIONS

In this paper we summarized the current state of MEBT systems upon beam commissioning. Most systems have been deployed successfully according to their design. In the near future, NPM cameras will be installed to measure beam size and position, and all the other systems will come online. MEBT beam properties characterisation and beam matching to DTL is of essential importance towards the next DTL cavities commissioning stages. The authors would like to thank T. Grandsaert for the 3D render of MEBT.

Content from this work may be used under the terms of the CC BY 4.0 licence (© 2021). Any distribution of this work must maintain attribution to the author(s), title of the work, publisher, and DOI

## REFERENCES

- [1] L. Bellan, “Space Charge and Electron Confinement in High Current Low Energy Transport Lines” presented at Proc. 31st Linear Accelerator Conference (LINAC’22), paper TUOPA08, this conference.
- [2] L. Neri *et al.*, “Beam Commission of the High Intensity Proton Source Developed at INFN-LNS for the European Spallation Source”, *J. Phys.: Conf. Ser.* 874, 0120372019, 2017 doi:10.1088/1742-6596/874/1/012037
- [3] L. Neri, “HSMDIS Performance On The ESS Ion Source”, presented at Proc. 31st Linear Accelerator Conference (LINAC’22), paper THPORI19, this conference.
- [4] M. Eshraqi *et al.*, “The ESS LINAC” in Proc. IPAC’14, Dresden, Germany, 2014, paper THPME043, pp 3320-3322
- [5] P. Hamel *et al.*, “ESS RFQ: Installation and Tuning at Lund”, in *Proc. IPAC’21*, Campinas, Brazil, May 2021, pp. 1372-1374. doi:10.18429/JACoW-IPAC2021-TUPAB016
- [6] F. Grespan, M. Comunian, A. Pisent, M. Poggi, C. R. Roncolato, and P. Mereu, “ESS DTL Design and Drift Tube Prototypes”, in *Proc. LINAC’14*, Geneva, Switzerland, Aug.-Sep. 2014, paper THPP087, pp. 1050-1052.
- [7] Fernández-Cañoto, D., Muñoz, J.L., Rueda, I. and Bustinduy, I., 2021. “Magnetic Analysis and Cross-Talk Fields for the ESS MEBT Quadrupole Magnet”, *Nuclear Instruments and Methods in Physics Research Section A: Accelerators, Spectrometers, Detectors and Associated Equipment*, 1014, p.165723.
- [8] I. Bustinduy *et al.*, “The ESS MEBT RF Buncher Cavities Conditioning Process”, in Proc. IPAC’21, Campinas, Brazil, May 2021, pp. 1107-1109. doi:10.18429/JACoW-IPAC2021-MOPAB356
- [9] B. Jones *et al.*, “Hardware Commissioning With Beam at the European Spallation Source: Ion Source to DTL1”, presented at LINAC’22, Liverpool, UK, 2022, paper TUPOJ010, this conference.
- [10] R. Miyamoto *et al.*, “Beam Commissioning of Normal Conducting Part and Status of ESS Project”, presented at LINAC’22, Liverpool, UK, 2022, paper MO1PA02, this conference.
- [11] A. Rodríguez Páramo *et al.*, “Design of the ESS MEBT Faraday Cup”, in *Proc. IBIC’19*, Malmö, Sweden, Sep. 2019, pp. 106-110. doi:10.18429/JACoW-IBIC2019-MOPP014